Optimizing Electrochemical Turbidity Removal from Water Using Response Surface Methodology

A. S. Khudier, M. J. Mawat, A. S. Dawood

Department of Civil Engineering, College of Engineering, University of Basrah, Basrah, Iraq.

ABSTRACT: Water turbidity, caused by suspended particulate matter, is a primary indicator of water quality and poses significant challenges for potable water production. This study investigates the optimization of the electrochemical coagulation (EC) process for removing kaolinite-induced turbidity from synthetic wastewater. By applying steel electrodes the impacts of 4 significant operational parameters (applied voltage (V), inter-electrode electrode distance (D), initial solution pH, and initial turbidity concentration (Co)) on turbidity removal efficiency were investigated carefully. The process was modeled and optimized using Response Surface Methodology (RSM) based on a factorial design. The analysis of variance (ANOVA) identified that voltage, pH and their quadratic terms V^2, pH^2), whereas the interaction between voltage and distance (V*D) as the most significant factors affecting turbidity removal ($p < 0.05$). The fitted quadratic model showed a high value of coefficient of determination (R^2 = 98.04%), indicating good predictive quality of the model. The model also estimated that the maximum turbidity removal of 98.9% was obtained under conditions of applied voltage of 25 V, electrode distance of 2 cm, pH (7 ± 1) and an initial turbidity value of 200 NTU. The results demonstrated that EC is an excellent process for turbidity reduction, and RSM is a powerful tool to optimize complex intersystem, multi-variable interactions associated with it, giving a strong basis for efficient design and operation of water treatment plants.

KEYWORDS: Electrocoagulation, Turbidity removal, Response surface methodology, Water treatment, Process optimization, Steel electrodes, Kaolinite.

[Received: Oct. 15, 2025; Revised: Feb. 12, 2026; Accepted: Mar. 17, 2026] Print ISSN: 0189-9546 | Online ISSN: 2437-2110

I INTRODUCTION

Driven by the increasing global population, industrialization, and climate change, the demand for clean and safe water is skyrocketing, while water scarcity and contamination are becoming among the most demanding issues of the 21st century (Mawat and Hamdan, 2023). Potable water is not only a basic human right but also a necessary condition for public health, economic development, and environmental sustainability (Boinpally et al., 2023). Among the various sources of water, surface water such as rivers, lakes and reservoirs are used to supply the majority of public water systems throughout the world (Mawat and Hamdan, 2023). Turbidity is a common problem in surface water.

Turbidity is a measure of the cloudiness or haziness of water, caused by the presence of finely divided and suspended matter such as clay, silt, finely divided inorganic and organic matter, soluble colored organic compounds, algae, and other microorganisms (Nair et al., 2014). Turbid water is unsightly and can be unhealthy. Suspended solids interfere with disinfection by shielding pathogens from disinfectants. Suspended solids can promote growth of bacteria, parasites, and viruses. High levels of turbidity support prolific growths of microorganisms that degrade water quality and pose risks to public health (Ghernaout & Ghernaout, 2011). The removal of turbidity is thus the first and most important step in any water treatment process. Conventional processes for removal of turbidity from water typically involve chemical coagulation, flocculation, sedimentation and filtration.

These techniques involve the addition of chemical coagulants, such as aluminum sulfate (alum) or ferric chloride, to water to remove dirt and other suspended particles. The coagulants neutralize the negative charges on particles and cause the particles to clump together into larger, more easily removable clumps called flocs. Although conventional coagulation/flocculation followed by sedimentation and filtration can be an effective method for the removal of turbidity, these processes have many disadvantages, such as large amount of chemicals must be handled, high costs for transportation and storage of chemicals, large volumes of chemical sludge are generated that must be disposed of, and costs associated with sludge disposal (Phu et al., 2025).

Moreover, the presence of residual coagulant ions (e.g., aluminum) in finished waters may cause health problems including Alzheimer's disease, Parkinson's disease, and muscle disorders. These concerns about coagulation/flocculation process have been driving researchers to explore other efficient and environmentally

*Corresponding author: *ahmed.khudier@uobasrah.edu.iq*

doi: http://doi.org/10.63746/njtd.v23i1.4095

friendly technologies. Electrochemical coagulation (EC) is a promising technology for turbidity abatement that offers several advantages over conventional chemical coagulation methods, which include high efficiency for removing pollutants, simplicity of equipment and easy operation, environmental compatibility of the process, and significantly lower amount of sludge generated.

EC is the generation of coagulants in the aqueous media by oxidation of a sacrificial anode material such as Fe or Al (Gafoor et al., 2021). An anode oxidation occurs when direct electric current passes and metal ions (Al^{3+} or Fe^{2+}/Fe^{3+}) are released in the aqueous media. In the meantime, reduction of water occurs at the cathode and hydrogen gas and OH^- are generated. The metal and hydroxide ions then react and form various monomeric and polymeric metal hydroxides which act as effective coagulants (Bani-Melhem et al., 2025). The in-situ formed hydroxides are characterized by a high surface area and hence have a high capacity to adsorb, destabilize and remove suspended particles and form compact flocs. Furthermore, electroflotation occurs with H_2 bubbles that are formed at the cathode, which helps in the removal of the flocs (Ghernaout & Ghernaout, 2011). EC has several benefits over other techniques such as low cost of equipment, easy automation, no chemical consumption, and compact and stable sludge formation (Phu et al., 2025).The EC process is controlled by various operating parameters which are highly inter-dependent.

Those are electrode material, applied voltage or current density, initial pH of the solution, inter-electrode distance, and the type and concentration of contaminants (Mousazadeh et al., 2023). Applied voltage is an important factor since it is directly related to the amount of coagulant production and bubble formation, which affects the efficiency of the treatment as well as the energy consumption (the most significant component of the operational cost) (Niazmand et al., 2020). Solution pH is another crucial factor because it determines the speciation of the metal hydroxides. For example, iron and aluminum have different soluble and insoluble species at different pH levels, which greatly influences the coagulation (Ebba et al., 2022). Thus, the optimization of those factors is necessary to achieve maximum treatment efficiency at minimum operational cost.The conventional method of optimization is a one-factor-at-a-time (OFAT) approach. The main disadvantages of the OFAT optimization are time-consuming, laborious, and inability to consider the interaction effects between variables, which may result in a false understanding of the process and less optimal solutions.

In order to tackle the aforementioned challenges, statistical experimental design techniques, such as Response Surface Methodology (RSM), have been broadly employed in modeling and optimization of environmental engineering processes (Nair et al., 2014). RSM is a set of statistical and mathematical techniques to design experiments, model responses and optimize the conditions of a response variable that is affected by several independent factors (Breig & Luti, 2021). RSM models the relationship between a response variable and one or more independent variables by fitting a polynomial model to the experimental data to describe the system under study and to identify the operating conditions that optimize the system performance. Although RSM has been employed for the optimization of EC for removal of a wide variety of pollutants including dyes (Bani-Melhem et al., 2025) and heavy metals (Ebba et al., 2022), there is a lack of knowledge on the application of RSM to model and optimize the most important operating parameters of EC (applied voltage, inter-electrode distance, initial pH, and initial turbidity) for the removal of kaolinite-induced turbidity using conventional steel electrodes. Therefore, the main objective of this research is to model and optimize the electrochemical removal of kaolinite-induced turbidity using Response Surface Methodology (RSM).

The specific objectives of this study are as follows: (1) to examine the linear and interaction effects of four operating variables, namely applied voltage, inter-electrode distance, initial pH, and initial turbidity concentration, on the removal efficiency; (2) to establish a robust quadratic regression model to predict the turbidity removal as a function of the aforementioned four operating parameters; and (3) to identify the optimal operating conditions for maximizing the turbidity removal. The outcome of this study will improve the understanding of the EC process and offers useful information for designing and operating efficient and economic water treatment systems.

II. MATERIAL AND METHODS

A. Materials and synthetic water preparation

The chemicals used in this study were of analytical grade. The synthetic turbid water was prepared from kaolinite clay ($Al_2Si_2O_5(OH)_4$), which is a major contributor to the natural water turbidity. The stock solution of kaolin clay was prepared by mixing an appropriate amount of kaolin powder in 100 mL of distilled water, followed by vigorous mixing for 30 min. The stock solution was diluted with tap water to prepare the initial desired turbidity concentrations (100, 200 and 300 NTU) used for this study which were measured using a turbidimeter. The initial pH of the solution was adjusted to the desired values (5, 7 and 9) by adding either 0.1 M HCl or 0.1 M NaOH.

B. Experimental setup

The electrocoagulation experiments were conducted in a 1 L glass beaker, which served as the batch reactor. The reactor was filled with 1 L of the prepared synthetic turbid water for each experimental run. A pair of steel plates was used as the sacrificial anode and cathode (Figure 1). The dimensions of each electrode were 15 cm in length, 3 cm in width, and 2.5 mm in thickness. The electrodes were positioned vertically and parallel to each other and inserted to a depth of 12 cm, giving an active surface area for each electrode of 36 cm 2. The inter-electrode distance was set according to the experimental conditions. The electrodes were linked to a DC power supply which enabled the applied voltage to be controlled accurately. Constant mixing of the solution at 200 rpm was performed to guarantee a homogenous solution and enhance mass transport with a magnetic stirrer. Runs were performed for 2 h and, after this time, the power supply was switched off and the solution left to settle for 1 h. The experimental setup scheme is

conceptually similar to that described for EC treatments in many studies.

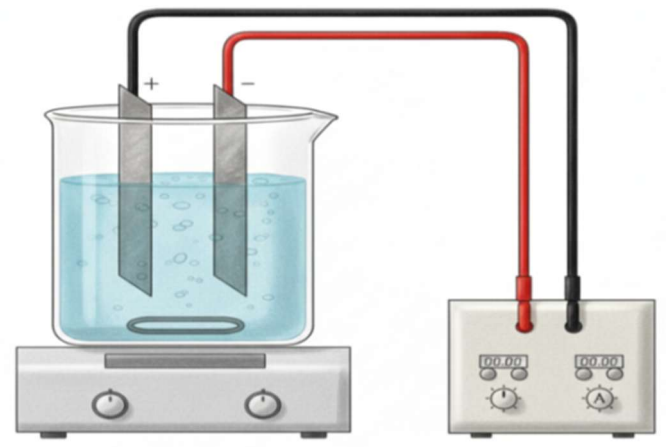

Figure 1 EC process arrangement, showing Perspex cell, pair of steel electrode, magnetic stirrer with its bar, and dc power supply

.

C. Analytical procedure

The water samples were taken from the supernatant for the determination of the final turbidity. At the end of the 1 h settling time, 50 mL of the sample solution was slowly taken from the supernatant with a pipette at a depth of 6 cm from the water surface (i.e., middle level of the submerged electrode zone) to keep the results consistent and not to disturb the sludge layer formed at the bottom. Turbidity was determined by turbidimeter. Turbidity removal efficiency (R%) was calculated as follows:

$$R(\%) = \left(\frac{C_o - C_f}{C_o} X\ 100\right) \quad (1)$$

Where C_o is the initial turbidity (NTU) and C_f is the final turbidity (NTU) of the treated water.

D. Experimental design and statistical analysis

Optimization of the process parameters: Response Surface Methodology (RSM) was used to study the effects of the operational variables on the turbidity removal efficiency and also to optimize the process parameters. In this study, a Central Composite Design (CCD) was used to assess the individual and interactive effects of four independent variables: applied voltage (V, X_1), inter-electrode distance (D, X_2), initial pH (X_3), and initial turbidity concentration (Co, X_4). CCD is a highly efficient design for fitting a second-order model and is ideal for quantifying the linear, quadratic, and interactive effects of the variables with a reasonable number of experimental runs (31 runs for four factors). Each variable was studied at three levels, as shown in Table 1. The response variable was the turbidity removal percentage (Y).

Table 1 Independent variables and their levels for the experimental design.

Independent Variable	Symbol	Unit	Level -1	Level 0	Level +1
Applied Voltage	X_1	V	5	15	25
Electrode Distance	X_2	cm	1	2	3
Initial pH	X_3	-	5	7	9
Initial Concentration	X_4	NTU	100	200	300

A total of 31 experimental runs were conducted based on the design matrix. The experimental data were analyzed using statistical software to fit a second-order polynomial regression model. The general form of the model is:

$$Y = \beta_o + \Sigma\, \beta_i X_i + \Sigma \beta_i X_i^2 + \Sigma\, \beta_{ij} X_i X_j + \varepsilon \quad (2)$$

where Y is the predicted response (turbidity removal %), β_0 is the constant coefficient, β_i, β_{ii}, and β_{ij} are the linear, quadratic, and interaction coefficients, respectively, X_i and X_j are the coded values of the independent variables, and ε is the model error. The statistical significance of the model and its terms was evaluated using Analysis of Variance (ANOVA) at a 95% confidence level (p-value < 0.05). The coefficient of determination (R^2) and the adjusted R^2 were used to evaluate the quality of model fit. Rendered plots in three-dimensional (3D) response surface and contour plots were created for the purpose of visualizing the interactive effects of the factors on the removal efficiency.

III RESULTS AND DISCUSSION

The experimental implementation of electrochemical turbidity removal was devised as per this Response Surface Methodology (RSM) model, which optimally adjusts four primary operation parameters: applied voltage (V), inter-electrode distance (D), initial solution pH, and initial concentration of turbidity (Co). The entire data set comprising 31 experimental runs was used to construct a predictive model and was also employed to interpret the relationships among operational variables that influence the process efficiency. The applications are represented with the means of statistical model analyses, regression diagnostics, and graphs of the interdependencies of parameters. The theoretical models of the electrochemical process of removing kaolinite-induced turbidity with the help of RSM were satisfactory; and were found to be useful in real applications. The proposed quadratic model exhibited good predictive properties with an R^2 of 98.04%, that is, the variances of process-related variables and the turbidity removal relationship are being adequately modeled. ANOVA analysis was a significant contributor to getting terms of reference on the importance of each variable whereby applied voltage was found to be the primary factor and also showed a pH level effect.

A. Model fitting and statistical analysis

The electrocoagulation process was represented numerically through Response Surface Methodology in order to examine the influence of applied voltage (V), electrode distance (D), pH, and initial concentration (Co) on turbidity removal efficiency. The design matrix and the corresponding experimental results for 31 runs are presented in Table 2.

Table 2 Experimental design matrix and results for turbidity removal

Run	V (V)	D (cm)	pH	Co (NTU)	Removal (%)
1	15	3	7	200	79.74
2	25	2	7	200	98.9
3	25	1	5	300	68.96
4	25	1	5	100	68.96
5	25	3	5	300	76.3
6	5	3	9	300	28
7	25	1	9	100	77.5
8	15	2	7	300	79.74
9	5	3	9	100	15.5
10	5	1	9	300	22.84
11	25	3	5	100	76.3
12	15	2	7	200	79.74
13	25	1	9	300	77.5
14	25	3	9	100	84.84
15	15	2	9	200	61.34
16	15	2	7	200	79.74
17	15	2	7	200	79.74
18	5	3	5	100	21
19	25	3	9	300	84.84
20	5	3	5	300	17
21	15	2	7	200	79.74
22	5	1	5	300	23
23	15	2	7	200	79.74
24	15	2	5	200	39.21
25	5	1	5	100	25
26	5	2	7	200	30.78
27	15	2	7	200	79.74
28	15	1	7	200	79.74
29	15	2	7	100	79.74
30	15	2	7	200	79.74
31	5	1	9	100	22.84

The data were fitted to a second-order polynomial model, and the final regression equation in terms of uncoded units was obtained as follows:

$$Removal\ (\%) = -250.7 + 5.14\,V - 24.5\,D + 88.2 - 0.229\,Co - 0.1130\,V^2 + 3.60\,D^2 - 6.467\,pH^2 + 0.000360\,Co^2 + 0.365\,V \times D + 0.0440\,V \times pH + 0.00065\,V \times Co + 0.772\,D \times pH - 0.0040\,D \times Co + 0.01106\,pH \times Co \quad (3)$$

The statistical significance of the model was validated by the Analysis of Variance (ANOVA), summarized in Table 3. The model F-value of 57.24 with a very low p-value (0.000) implies that the model is highly significant. The quality of the fit was confirmed by the high coefficient of determination (R^2 = 98.04%), which indicates that 98.04% of the variability in the turbidity removal can be explained by the model. The adjusted R^2 (96.33%) is also high and in reasonable agreement with the R^2, further attesting to the model's accuracy.

Table 3 Analysis of Variance (ANOVA) for the quadratic model.

Source	DF	Adj SS	Adj MS	F-Value	P-Value
Model	14	22629	1616.4	57.24	0
Linear	4	15644.9	3911.2	138.5	0
V	1	15314.8	15314.8	542.31	0
D	1	0	0	0	0.99
pH	1	324	324	11.47	0.004
Co	1	6	6	0.21	0.651
Square	4	6632.5	1658.1	58.71	0
V×V	1	331.6	331.6	11.74	0.003
pH×pH	1	1736.6	1736.6	61.5	0
2-Way Interaction	6	351.7	58.6	2.08	0.114
V×D	1	213.5	213.5	7.56	0.014
Error	16	451.8	28.2		
Total	30	23080.8			

Based on the p-values, the linear terms for voltage (V) and pH are highly significant ($p < 0.01$). The quadratic terms V×V and pH×pH are also highly significant ($p < 0.01$), indicating a strong curvature in the response surface. The interaction term V×D is significant ($p = 0.014$), suggesting that the effect of voltage on turbidity removal depends on the electrode distance. The other linear, quadratic, and interaction terms were found to be statistically insignificant ($p > 0.05$).

For the model diagnostic, a high value of R^2 is not a guarantee for the model to be adequate. To check the adequacy of the model, normal probability plot of the residuals and plot of residuals versus the predicted response were drawn (Figure 2). In the normal probability plot of residuals, it is observed that the points on this plot lie approximately along a straight line, suggesting that the assumption of normality is satisfied. Figure 2a shows the plot of residuals versus the predicted response. It is observed that the points are randomly dispersed around the horizontal line. This suggests that the model satisfies the assumption of constant variance. The diagnostic plots reasonably support the model adequacy and the lack of bias or systematic error in the predictions of the regression model.

B. Effect of applied voltage

Applied voltage was obviously the dominant variable among all the factors with the lowest p-value (<0.001) and the largest F-value (542.31) in the ANOVA table. The removal efficiency was enhanced significantly from as low as ~15-30% at 5 V to over 98% at 25 V. The positive dependency is clearly in line with the electrocoagulation mechanism. The anode dissolution is proportional to the electrical charge passed through the solution (Faraday's law). According to Faraday's law, the mass of electrode material dissolved is directly proportional to the total electric charge passed through the system. In our potentiostatic (constant voltage) setup, a higher applied voltage drives a higher current density, which is the primary force for coagulant production (Niazmand et al., 2020). In the case of our potentiostatic system, higher applied voltage results in higher current density which is the driving force for coagulant production (Niazmand et al., 2020). This consequently enhances the rate of Fe^{2+}/Fe^{3+} ion production at the anode (Equation 4).

$$\text{Anode: } Fe(s) \rightarrow Fe^{2+}(aq) + 2e^{-} \quad (4)$$

These in-situ generated iron ions hydrolyze to form a variety of metal hydroxide species such as $Fe(OH)_2$ and $Fe(OH)_3$ and various polymeric hydroxo complexes (Ghernaout & Ghernaout, 2011). These hydroxides act as coagulants that neutralize the negative surface charge of colloidal kaolinite particles and then trap them through the "sweep flocculation" mechanism (Kuokkanen et al., 2013). Hence, a higher voltage would lead to more abundant and faster production of these coagulating agents, resulting in more extensive destabilization and aggregation of suspended particles. Moreover, a higher voltage enhances the rate of hydrogen gas evolution at the cathode which can improve the floc separation through electroflotation (Bleeke et al., 2015). The significant negative quadratic term for voltage (V×V, p=0.003) indicates that although the increase in voltage is very beneficial, there might be an optimum point where the increment in removal efficiency would not be justified by the increased energy cost. This suggests a point of diminishing returns, where further increases in voltage lead to progressively smaller gains in removal efficiency while significantly increasing operational costs due to higher energy consumption ($I = V/R$).

C. Effect of pH

Initial pH was the second factor in order of significance ($p = 0.004$). Its highly significant quadratic term (pH×pH, $p < 0.001$) indicates a non-linear, parabolic relationship with turbidity removal, implying the existence of an optimal pH value. The process efficiency is declined at both low and

high pH values. The significant negative quadratic term (pH × pH) indicates the existence of a maximum for the process at certain pH value, and decline of the efficiency with further deviations in both directions from that point. This is because of the iron hydroxide speciation and surface charge of the kaolinite particles (Chen, 2004). At lower pH values (e.g., < 6), iron is present mainly in the form of soluble cations such as Fe^{2+} and Fe^{3+} which is not suitable for sweep flocculation (Mollah et al., 2001). In this acidic range, the coagulant species are less effective at enmeshing suspended particles. In the near neutral pH range (6 to 9), iron is precipitated as insoluble hydroxides such as $Fe(OH)_2$ and $Fe(OH)_3$, which are mainly responsible for the entrapment and removal of colloidal particles (Mousazadeh et al., 2023). The highest efficiency observed at pH 7 in this study was likely to be due to the optimal formation of amorphous and insoluble iron hydroxides, which is the ideal pH value for coagulation process. At higher pH values (> 9), soluble anionic hydroxo-complexes like $[Fe(OH)_4]^-$ can be formed, which decreases the amount of solid precipitate available for coagulation and can even re-stabilize particles through charge reversal, thereby decreasing the removal efficiency (Kobya et al., 2003).

D. Effect of electrode distance and initial concentration

The main effects of electrode distance (D) and initial turbidity concentration (Co) were found to be statistically insignificant ($p > 0.05$), as shown in Table 3. However, discussion of these factors is warranted due to significant interactions and the practical implications of the findings. While the main effect of electrode distance (D) was not significant ($p = 0.990$), but its interaction with voltage (V×D) was ($p = 0.014$), meaning that the effect of distance is dependent on the applied voltage. Inter-electrode distance influences the internal (ohmic) resistance of the cell. According to Ohm's law, for a fixed voltage, increasing the distance, results in increasing the resistance and decreasing the current (the driving force for coagulant generation) (Hakizimana et al., 2017). This resistance increase requires more energy (ohmic loss) for the same current density. The interaction of V×D indicates that for lower voltages, where the current is low, the effect of distance is minimal. For higher voltages, where the system is more sensitive to the ohmic resistance, distance becomes a critical parameter for efficiency and energy consumption. In practice, the distance should always be minimized for energy saving as long as mixing is ensured and there is no risk of short-circuit (Gafoor et al., 2021).

Interestingly, the initial turbidity concentration (Co) was also not significant ($p = 0.651$) for removal efficiency in the range 100 to 300 NTU. This is an interesting result as it highlights the robustness of the process. In EC, the coagulant dose is determined by the current and time (Faraday's law) and not by the initial concentration of pollutant, unlike chemical coagulation (Chen, 2004). This result implies that the quantity of coagulant produced (especially at higher voltages) was always enough to effectively destabilize the particles available, thus the initial load was not a limiting factor in this range. This demonstrates a key advantage of EC: its performance is less sensitive to fluctuations in influent pollutant concentration compared to conventional coagulation where coagulant dosing must be constantly adjusted. At much higher initial turbidities, the system may become limited by the amount of coagulant, in which case initial concentration may become significant.

E. Primary interaction analysis

This section focuses on the interaction between the operational variables on the response, i.e., removal efficiency. This is carried out with 3D surface and 2D contour plots to provide both qualitative and quantitative visualizations of these interactions.

1) Effect of voltage and distance

The interaction between applied voltage and electrode distance is visualized in Figure 2. The 3D surface plot (Figure 2a) illustrates a steep incline in removal efficiency as voltage increases, confirming its dominant role. The effect of distance appears more nuanced. For a more precise interpretation, the 2D contour plot (Figure 2b) shows that the highest removal efficiency (>90%) is achieved in the region of high voltage (V > 20 V) and an intermediate electrode distance (D ≈ 1.5-2.5 cm). At a fixed high voltage (e.g., 25 V), efficiency is high across the tested distances, but the peak is centered around 2 cm. This suggests a trade-off: a smaller distance reduces ohmic resistance and energy loss, but a very small distance might impede mass transfer and bubble-induced mixing. Conversely, a larger distance increases ohmic resistance, reducing current density and coagulant production. The optimal distance of 2 cm likely represents the best balance between minimizing ohmic resistance and allowing for effective hydrodynamics within the reactor. The significant V×D interaction term ($p=0.014$) is visually confirmed by the non-parallel contour lines.

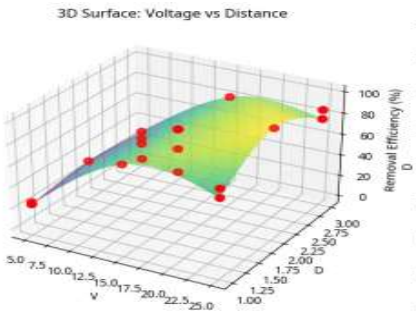

(a) 3D Surface:Voltage vs Distance

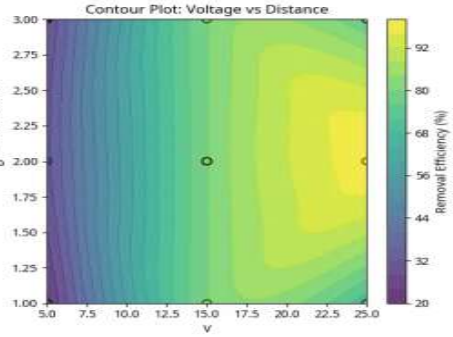

(b) Contour plot: Voltage vs Distance

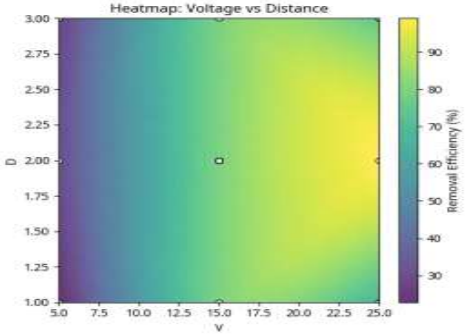

(c) Heatmap: Voltage vs Distance

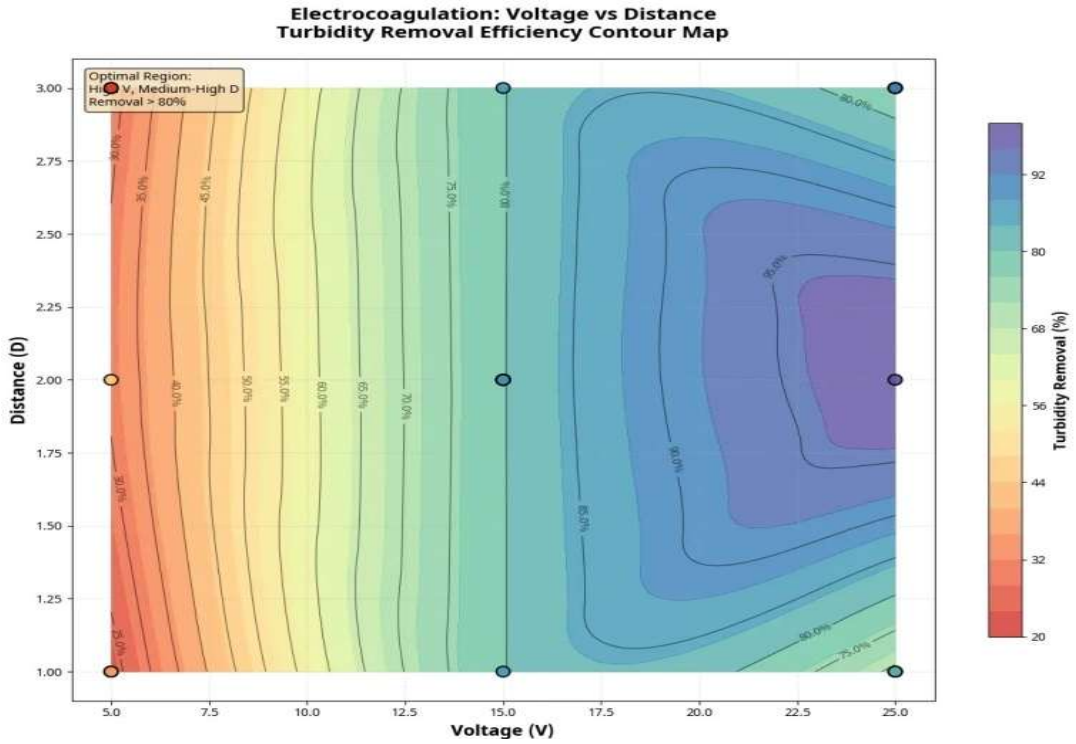

(d) Electrocoagulation: voltage vs Distance, Turbidity removal efficiency contour map

Figure 2 Interaction effect of applied voltage (v) and electrode distance (D) on turbidity removal; efficiency, (a) 3D surface plot, (b) 2D contour plot, (c) Heatmap analysis, and (d) contour plot.

2) Effect of voltage (V) and pH

Figure 3 illustrates the interaction between applied potential and initial pH. As can be seen in the response surface (Figure 3a), there is a distinct ridge where the maximum removal efficiencies are observed, and a decline in efficiency is noticed before and after this ridge. The contour plot (Figure 3b) gives a better representation of the removal efficiencies, indicating that the maximum removal efficiencies (>90%) are located in the high potential region (V > 20 V) for a narrow pH range (pH 6.5−7.5). This result is in agreement with the ANOVA analysis that indicated a significant quadratic effect for pH. It can be observed that, at the lowest potential (5 V), removal is poor regardless of pH. However, at higher potentials, the iron removal process is very efficient only at the optimal pH values, for which the iron species are mostly precipitated as $Fe(OH)_2$ and $Fe(OH)_3$. Outside this window, even at high voltage, efficiency is compromised due to the formation of less effective soluble iron species (at low pH) or anionic complexes (at high pH). The optimal point (98.9% removal) is located at V=25 and pH=7, residing in the center of this high-efficiency zone.

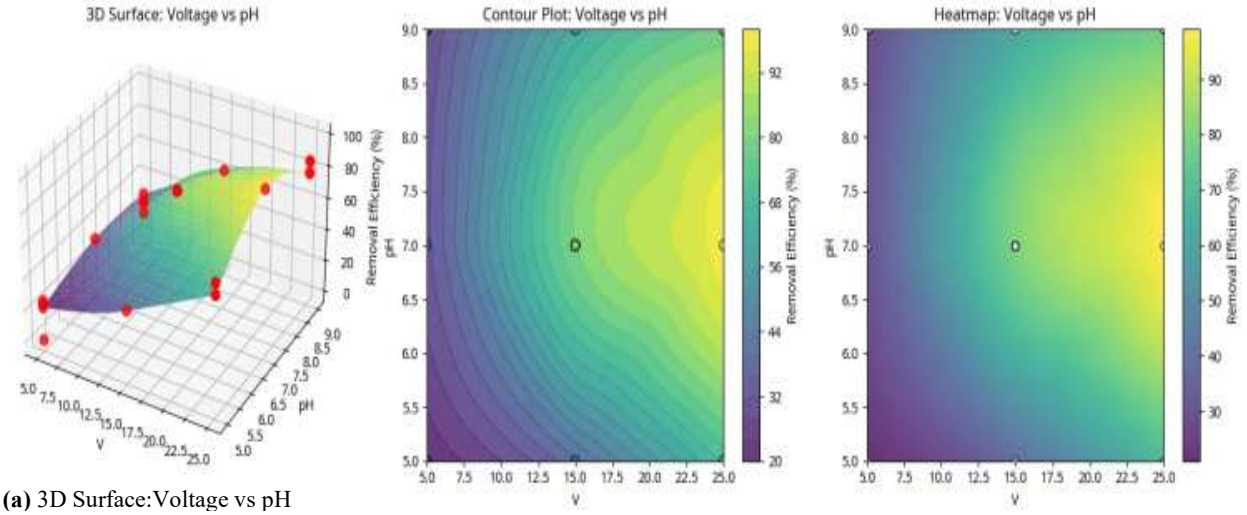

(a) 3D Surface:Voltage vs pH

(b) Contour plot:Voltage vs pH

(c) Heatmap: Voltage vs pH

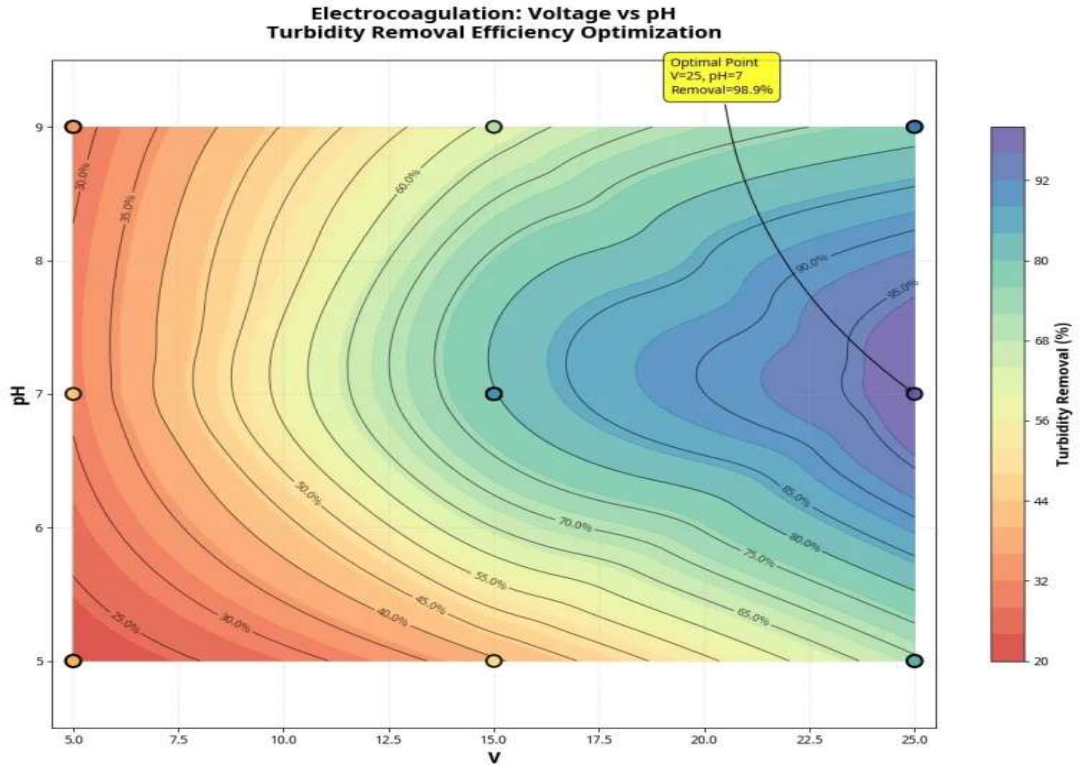

(d) Electrocoagulation: voltage vs pH, Turbidity removal efficiency Optimization

Figure 3 Visualization of the interaction between applied voltage (V) and initial pH on removal efficiency, (a) 3D Surface: Voltage vs pH, (b) Contour plot: Voltage vs pH, (c) Heatmap: Voltage vs pH, and (d) Contour plot.

3) Effect of voltage (V) and initial turbidity (Co)

AThe relationship between voltage and initial turbidity is shown in Figure 4. The 3D surface (Figure 4a) and 2D contour (Figure 4b) plots both demonstrate that voltage is the overwhelming factor, with removal efficiency increasing dramatically with higher voltage across the entire range of initial turbidity (100-300 NTU). The contour lines are nearly vertical, indicating that for any given voltage, the change in initial turbidity has a minimal impact on removal efficiency. This visual evidence strongly supports the ANOVA result that the main effect of initial concentration (Co) and its interaction with voltage were not statistically significant ($p > 0.05$). This implies that under the tested conditions, particularly at voltages above 15 V, the amount of coagulant generated in-situ was sufficient to treat the turbidity load

effectively, regardless of whether it was 100, 200, or 300 NTU. This highlights the robustness of the EC process.

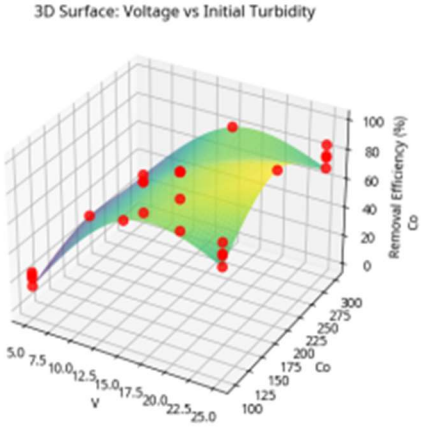

(a) 3D Surface: Voltage vs Initial Turbidity

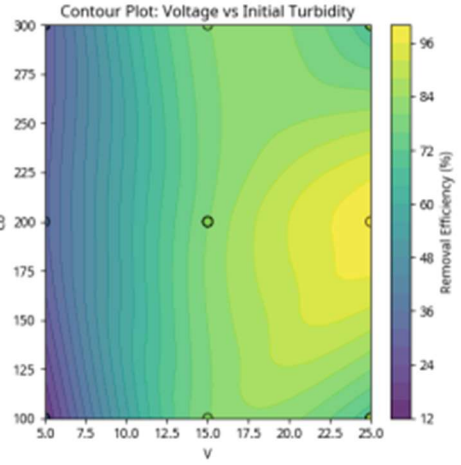

(b) Contour plot: Voltage vs Initial Turbidity

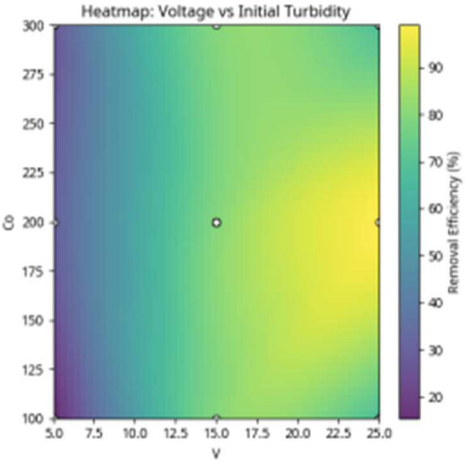

(c) Heatmap: Voltage vs Initial Turbidity

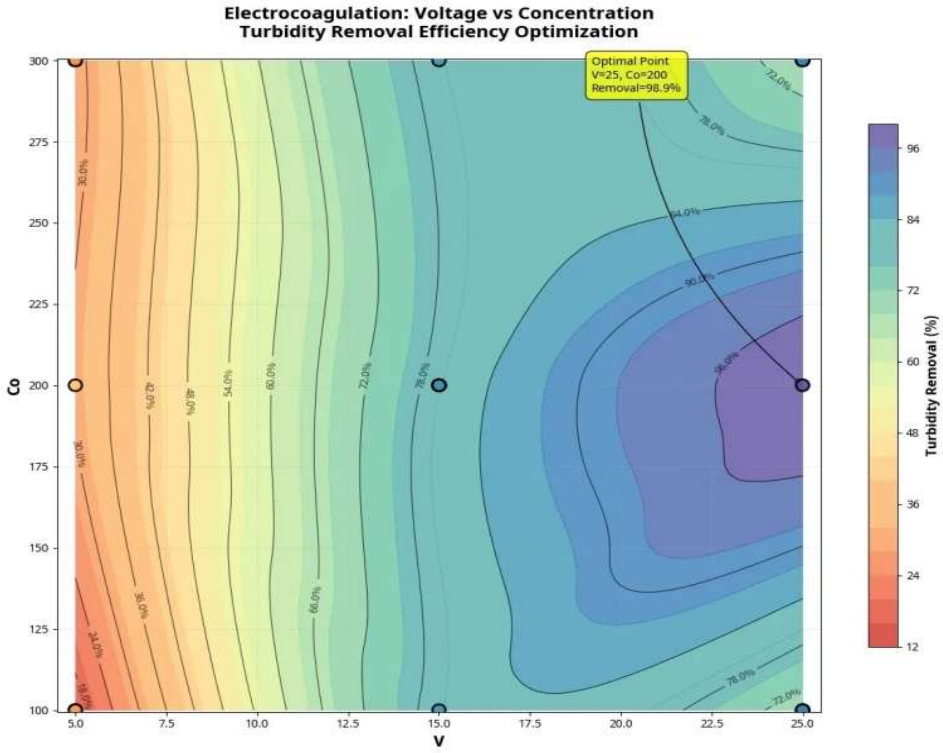

(d) Electrocoagulation: voltage vs Concentration, Turbidity removal efficiency Optimization

Figure 4 Analysis of how applied voltage (V) and initial turbidity concentration (Co) affect removal efficiency, (a) 3D Surface: Voltage vs Initial Turbidity, (b) Contour plot: Voltage v Initial Turbidity, (c) Heatmap: Voltage v Initial Turbidity, and (d) Contour Plot.

4) Effect of distance and pH

Figure 5 illustrates the combined influence of electrode distance and pH. The 3D surface (Figure 5a) and 2D contour (Figure 5b) plots both show a distinct optimal region. The highest removal efficiencies are centered around a neutral pH (≈7) and a smaller electrode distance (≈1.5-2.5 cm). The contour plot clearly shows that efficiency drops significantly as pH moves into the acidic or alkaline ranges, regardless of the distance. Similarly, for any given pH, increasing the distance beyond 2.5 cm tends to lower the removal efficiency, likely due to increased ohmic resistance. Although the interaction term D×pH was not statistically significant ($p > 0.05$), the plots visually suggest that maintaining a near-neutral pH is critical, and within that optimal pH range, a smaller electrode distance is preferable

for achieving maximum efficiency. The optimal point of D=2 cm and pH=7 is located at the peak of the response surface.

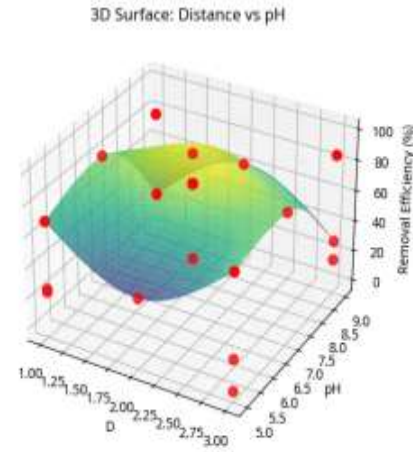

(a) 3D Surface: Distance vs pH

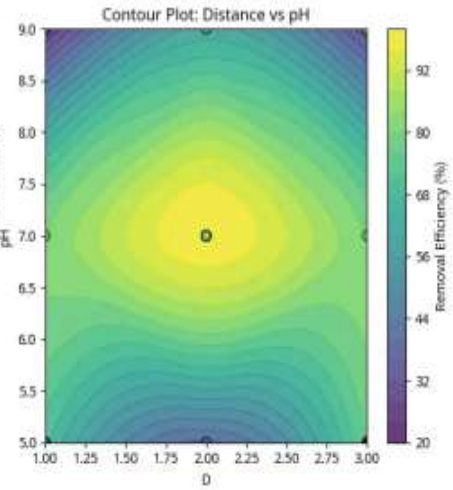

(b) Contour plot: Distance vs pH

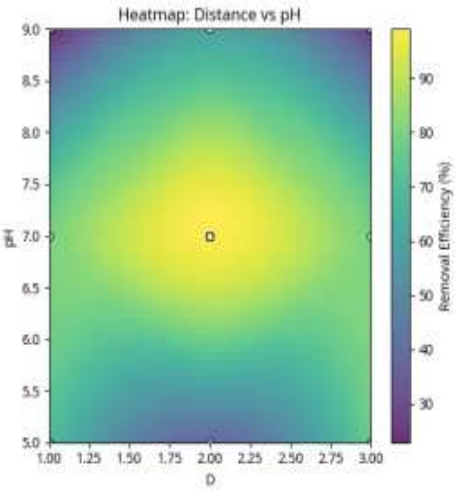

(c) Heatmap: Distance vs pH

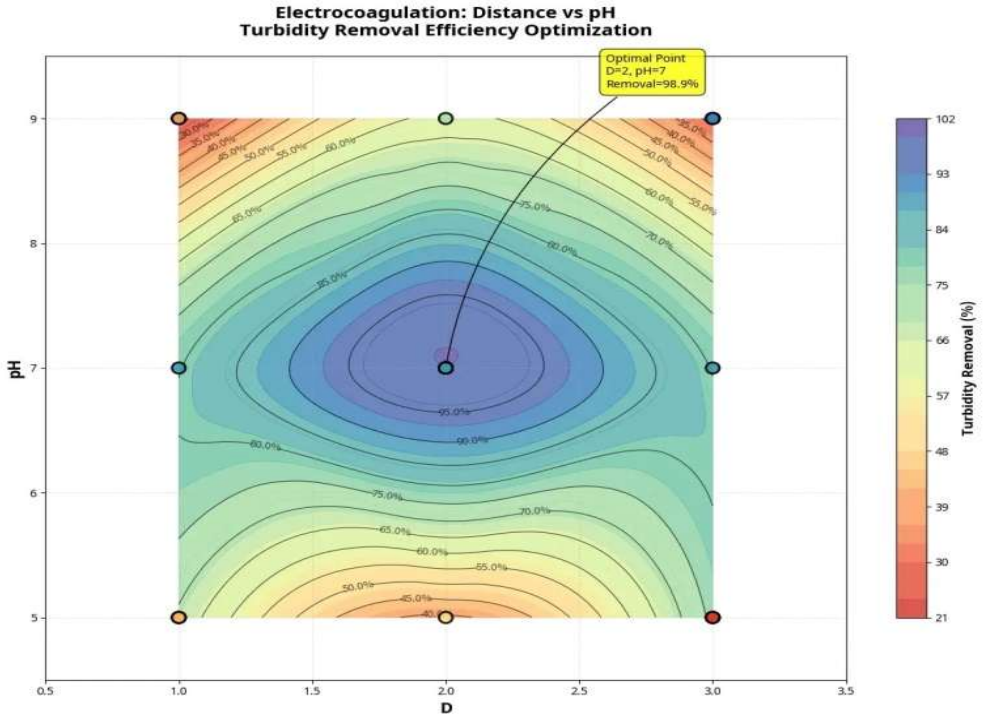

(d) Electrocoagulation: Distance vs pH, Turbidity removal efficiency Optimization

Figure 5 Visualization of the interaction between electrode distance (D) and initial pH on removal efficiency, (a) 3D Surface: Distance vs pH, (b) Contour plot: Distance vs pH, (c) Heatmap: Distance vs pH, and (d) Contour Plot.

5) Effect of distance (D) and initial turbidity (Co)

The interaction between electrode distance and initial turbidity is depicted in Figure 6. Both the 3D surface plot (Figure 6a) and the 2D contour plot (Figure 6b) show relatively flat surfaces, which aligns with the ANOVA results indicating that neither D nor Co were significant main effects, and their interaction was also insignificant. However, a subtle trend can be observed from the contour plot (Figure 6b). The highest efficiency region is found at an intermediate distance (around 2 cm) and an intermediate initial concentration (around 200 NTU). The efficiency decreases slightly at larger distances (D=3 cm), likely due to increased ohmic resistance. The relative insensitivity of the removal efficiency to these two parameters within the tested ranges further underscores the robustness of the EC process, which

is primarily dictated by the electrochemically controlled coagulant dosage.

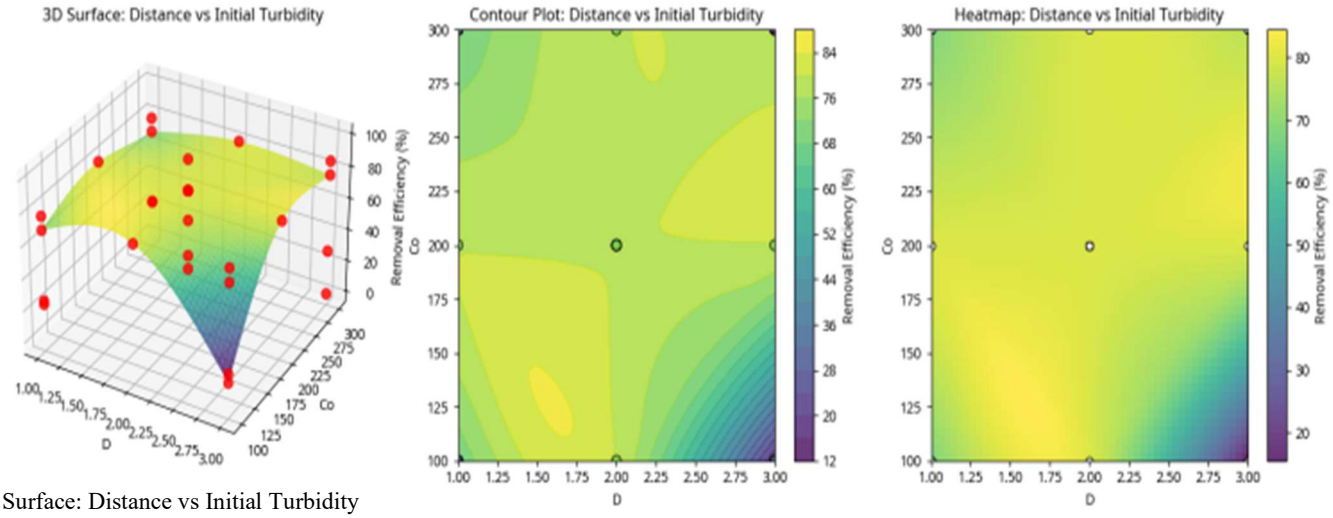

(a) 3D Surface: Distance vs Initial Turbidity

(b) Contour plot: Distance vs Initial Turbidity

(c) Heatmap: Distance vs Initial Turbidity

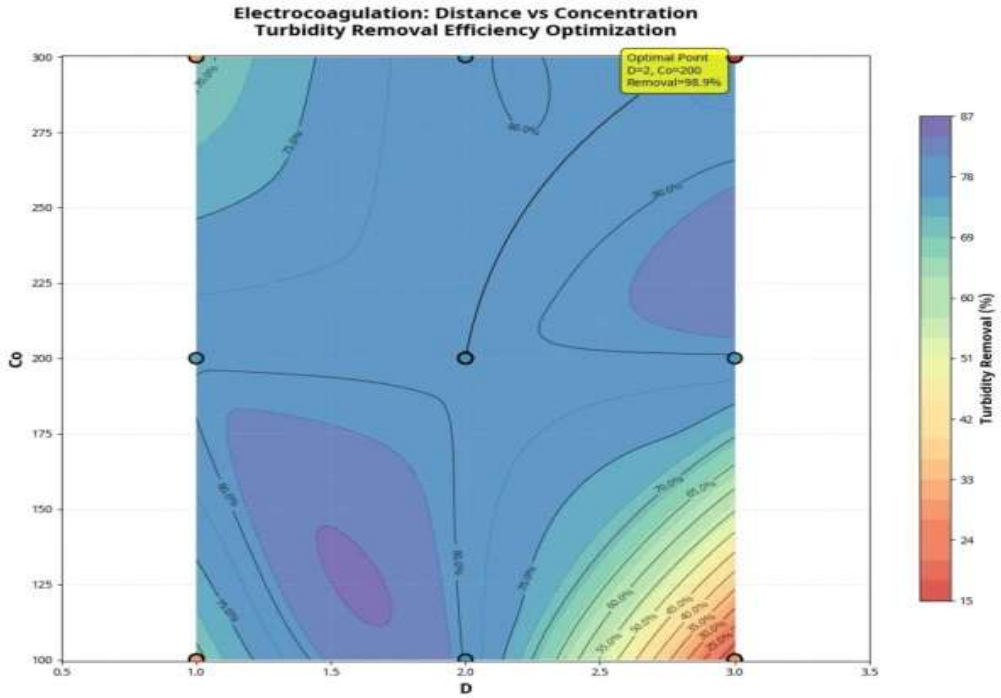

(d) Electrocoagulation: Distance vs Concentration, Turbidity removal efficiency Optimization

Figure 6 Analysis of electrode distance (D) and initial turbidity (Co) effects on removal efficiency, (a) 3D Surface: Distance vs Initial Turbidity, (b) Contour plot: Distance vs Initial Turbidity, (c) Heatmap: Distance vs Initial Turbidity, and (d) Contour Plot.

6) Effect of pH and initial turbidity (Co)

Finally, the interaction between pH and initial turbidity is shown in Figure 7. The significant impact of pH on the system is clear from the response surface plot (Figure 7a) and contour plot (Figure 7b). There is a sharp ridge in the response surface plot running along the pH axis peaking at pH 7. The efficiency falls significantly at pH 5 and pH 9. The contour plot has almost horizontal lines which signify that regardless of the initial turbidity concentrations (100-300 NTU), the removal efficiency is almost constant for any specific value of pH.

This again confirms the ANOVA findings where pH was a highly significant factor while Co was not. The optimal performance is consistently achieved at a neutral pH, which facilitates the formation of the most effective iron hydroxide

precipitates for sweep flocculation, irrespective of the initial particle load in the water.

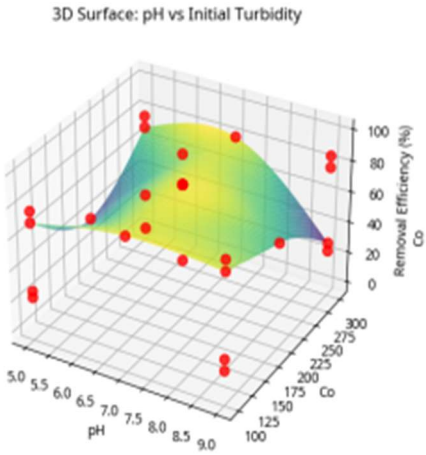

(a) 3D Surface: pH vs Initial Turbidity

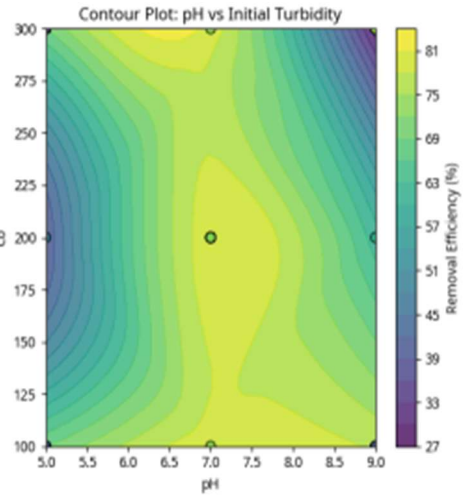

(b) Contour plot: pH vs Initial Turbidity

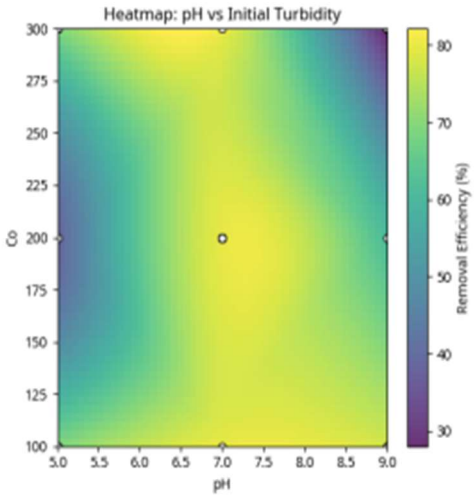

(c) Heatmap: pH vs Initial Turbidity

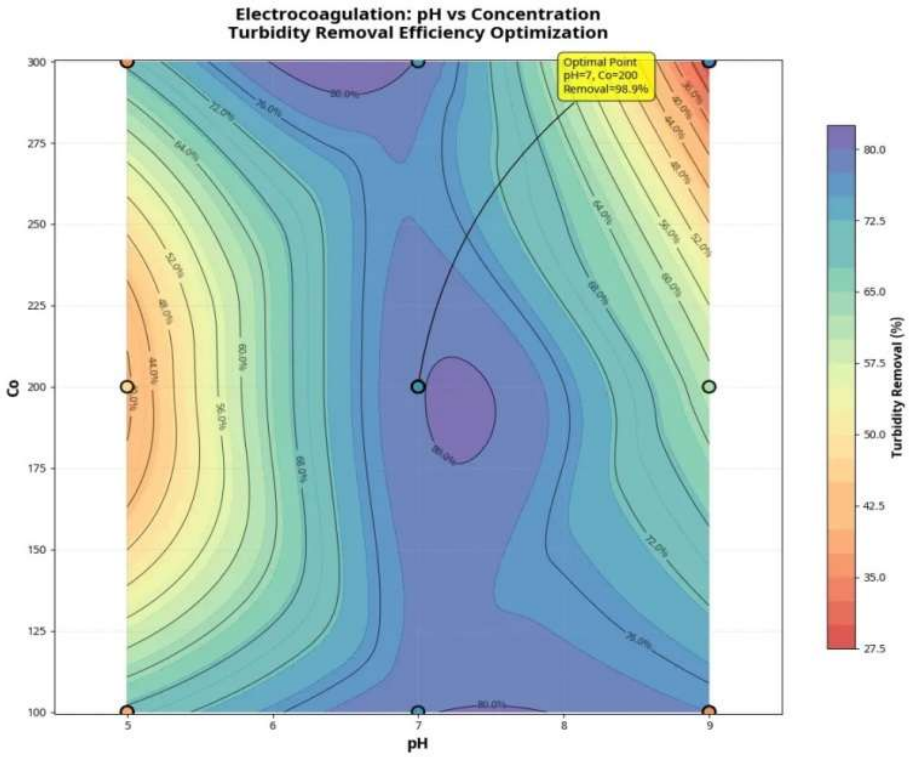

(d) Electrocoagulation: pH vs Concentration, Turbidity removal efficiency Optimization.

Figure 7 Analysis showing the interaction effects of initial pH and initial turbidity (Co) on removal efficiency, (a) 3D Surface: pH vs Initial Turbidity, (b) Contour plot: pH vs Initial Turbidity, (c) Heatmap: pH vs Initial Turbidity, (d) Contour Plot.

F. Optimization and model validation

The main objective of this study is the optimization of EC. The RSM was able to achieve the highest removal efficiency of turbidity. In the experimental study, the highest removal (98.9%) was found at 25 V, 2 cm distance, pH 7, and 200 NTU. This is in good agreement with RSM results, where the highest efficiency was predicted at the highest voltage level and neutral pH. Therefore, the capability of RSM in achieving the real optimal point in a multivariable system, which is very difficult to predict using conventional OFAT, is demonstrated in the present study The results are consistent with other studies like Ebba et al. (2022) identified the best operating conditions for textile wastewater treatment at pH 7.5 and a specific current, reaching high removal rates

of turbidity and COD. Similarly, Bani-Melhem et al. (2025) optimized EC for gray water treatment using RSM and obtained 98.5% of turbidity removal from the system at current density of 15.5mA/cm².

The repeatability of such results in different wastewaters enhances the reliability of EC process and RSM optimization methodology. The achievement of statistically significant high R^2 value (98.04%) of quadratic model implies that RSM is adequate to model and optimize the complicated and multiple quest environmental process such as electrocoagulation. Use of such RSM designs, specifically Central Composite Design (CCD), or Box-Behnken design (BBD) not only helps in efficient utilization of the experimental domain, but can also facilitate recognition and quantification of interaction which would be overlooked by the conventional one-factor-at-a- time experiments (Bezerra et al., 2008; Sarrai et al., 2016). Close correspondence between the model predicted optimum and that of the best experimental run confirms predictive ability of this model. This powerful predictive ease simulation greatly facilitates process up-scaling by providing an optimal operating set-point without the need for intensive and expensive trial-and-error experiments (Nair et al., 2014). The result also reveals a convenient operation roadmap, showing that at the highest voltage, an almost neutral pH condition while a relatively low electrode gap is optimally effective in attaining high turbidity removal.

IV. CONCLUSION

The objective of the present study is to apply the Response Surface Methodology (RSM) to optimize the electrochemical coagulation (EC) process using steel electrodes for the removal of kaolinite from synthetic wastewater. The use of RSM with Central Composite Design (CCD) is a powerful tool for modeling multivariable systems, overcoming the disadvantages of classical one-factor-at-a-time methods. The main drawback of this study is that it is conducted at a laboratory scale using synthetic wastewater which is far from the real conditions of water samples. The results indicated that a quadratic model was able to predict the turbidity removal efficiency with a high coefficient of determination (R^2 = 98.04%). The analysis of variance (ANOVA) results showed that applied voltage and initial pH were the two most significant variables, and their quadratic terms were also significant. The maximum predicted turbidity removal efficiency of 98.9% was obtained at an applied voltage of 25 V, inter-electrode distance of 2 cm, initial pH of 7, and initial turbidity of 200 NTU.

To fill the knowledge gap between the laboratory results and the practical application, a techno-economic study in terms of energy consumption (kWh/m^3), determination of volume and characteristics of the sludge generated, and model validation using real surface water samples are suggested for future studies. Moreover, the use of strategies such as reversing the polarity of the electrodes at regular intervals to avoid passivation is suggested for a stable long-term performance of the electrocoagulation process.

REFERENCES

Alzaidy, H. K., Al Khatib, F. M., & Dawood, A. S. (2023). The use of a pumice stone in removal of petroleum hydrocarbons from industrial wastewater through coagulation and flocculation. Environmental Health Engineering and Management Journal, 10(2), 141-147. https://doi.org/10.34172/EHEM.2023.16

Bani-Melhem, K., Alnaief, M., Al-Qodah, Z., Al-Shannag, M., Elnakar, H., AlJbour, N,& Ezelden, E. (2025). On the performance of electrocoagulation treatment of high-loaded gray water: kinetic modeling and parameters optimization via response surface methodology. Applied Water Science, 15(5), 1-21. https://doi.org/10.1007/s13201-025-02451-z.

Bezerra, M. A., Santelli, R. E., Oliveira, E. P., Villar, L. S., & Escaleira, L. A. (2008). Response surface methodology (RSM) as a tool for optimization in analytical chemistry. Talanta, 76(5), 965-977. https://doi.org/10.1016/j.talanta.2008.05.019.

Bleeke, F., Quante, G., Winckelmann, D., & Klöck, G. (2015). Effect of voltage and electrode material on electroflocculation of Scenedesmus acuminatus. Bioresources and Bioprocessing, 2(1), 36. https://doi.org/10.1186/s40643-015-0064-6

Boinpally, S., Kolla, A., Kainthola, J., Kodali, R., & Vemuri, J. (2023). A state-of-the-art review of the electrocoagulation technology for wastewater treatment. Water Cycle, 4, 26-36. https://doi.org/10.1016/j.watcyc.2023.01.001.

Breig, S. J. M., & Luti, K. J. K. (2021). Response surface methodology: A review on its applications and challenges in microbial cultures. Materials Today: Proceedings, 42, 2277-2284. https://doi.org/10.1016/j.matpr.2020.12.316.

Chasib, S. A., Azeez, N. M., & Dawood, A. S. (2021, April). Optimization of composite polymer dosing and pH in wastewater treatment plants. In IOP Conference Series: Earth and Environmental Science (Vol. 722, No. 1, p. 012038). IOP Publishing. https://doi.org/:10.1088/1755-1315/722/1/012038.

Chen, G. (2004). Electrochemical technologies in wastewater treatment. Separation and purification Technology, 38(1), 11- 41. https://doi.org/10.1016/j.seppur.2003.10.006.

Daneshvar, N., Oladegaragoze, A., & Djafarzadeh, N. (2006). Decolorization of basic dye solutions by electrocoagulation: an investigation of the effect of operational parameters. Journal of hazardous materials, 129(1-3), 116-122. https://doi.org/10.1016/j.jhazmat.2005.08.033 .

Dawood, A. S., & Li, Y. (2013). Modeling and optimization of new flocculant dosage and pH for flocculation: removal of pollutants from wastewater. Water, 5(2), 342-355. https://doi.org/10.3390/w5020342 .

Dawood, A. S., & Li, Y. L. (2012). Response surface methodology (RSM) for wastewater flocculation by a novel (AlCl3-PAM) hybrid polymer. Advanced Materials Research, 560, 529-537.

https://doi.org/10.4028/www.scientific.net/AMR.560-561.529.

Ebba, M., Asaithambi, P., & Alemayehu, E. (2022). Development of electrocoagulation process for wastewater treatment: optimization by response surface methodology. Heliyon, 8(5). https://doi.org/10.1016/j.heliyon.2022.e09383.

Gafoor, A., Ali, N., Kumar, S., Begum, S., & Rahman, Z. (2021). Applicability and new trends of different electrode materials and its combinations in electro coagulation process: a brief review. Materials Today: Proceedings, 37, 377-382. https://doi.org/10.1016/j.matpr.2020.05.379 .

Ghernaout, D., Naceur, M. W., & Ghernaout, B. (2011). A review of electrocoagulation as a promising coagulation process for improved organic and inorganic matters removal by electrophoresis and electroflotation. Desalination and Water Treatment, 28(1-3), 287-320. https://doi.org/10.5004/dwt.2011.1493.

Hakizimana, J. N., Gourich, B., Chafi, M., Stiriba, Y., Vial, C., Drogui, P., & Naja, J. (2017). Electrocoagulation process in water treatment: A review of electrocoagulation modeling approaches. Desalination, 404, 1-21. https://doi.org/10.1016/j.desal.2016.10.011

Holt, P. K., Barton, G. W., & Mitchell, C. A. (2005). The future for electrocoagulation as a localised water treatment technology. Chemosphere, 59(3), 355-367. https://doi.org/10.1016/j.chemosphere.2004.10.023.

Jaiswar, V. K., & Saroha, A. K. (2025). Effect of different electrode configuration modes on the performance of electrocoagulation. Journal of the Indian Chemical Society, 102(2), 101569. https://doi.org/10.1016/j.jics.2025.101569

Kobya, M., Can, O. T., & Bayramoglu, M. (2003). Treatment of textile wastewaters by electrocoagulation using iron and aluminum electrodes. Journal of hazardous materials, 100(1-3), 163-178. https://doi.org/10.1016/S0304-3894(03)00102-X.

Kuokkanen, V., Kuokkanen, T., Rämö, J., & Lassi, U. (2013). Recent applications of electrocoagulation in treatment of water and wastewater-a review. Green and Sustainable Chemistry, 3(2), 89-121. http://dx.doi.org/10.4236/gsc.2013.32013.

Mawat, M. J., Hamdan, A., N. (2023). Simulation of 2D Depth Averaged Saint Venant Model of Shatt Al Arab River South of Iraq. International Journal of Design & Nature and Ecodynamics, Vol. 18, No. 3, June, 2023, pp. 583-592. https://doi.org/10.18280/ijdne.180310.

Mawat, M. J., Hamdan, A., N. (2023). Integration of numerical models to simulate 2D hydrodynamic/water quality model of contaminant concentration in Shatt Al-Arab River with WRDB calibration tools. Open Engineering, vol. 13, no. 1, 2023, pp. 20220416. https://doi.org/10.1515/eng-2022-0416 .

Mollah, M. Y., Morkovsky, P., Gomes, J. A., Kesmez, M., Parga, J., & Cocke, D. L. (2004). Fundamentals, present and future perspectives of electrocoagulation. Journal of hazardous materials, 114(1-3), 199-210. https://doi.org/10.1016/j.jhazmat.2004.08.009

Mousazadeh, M., Khademi, N., Kabdaşlı, I., Rezaei, S., Hajalifard, Z., Moosakhani, Z., & Hashim, K. (2023). Domestic greywater treatment using electrocoagulation-electrooxidation process: optimisation and experimental approaches. Scientific Reports, 13(1), 15852. https://doi.org/10.1038/s41598-023-42831-6

Nabeel, M., & Dawood, A. S. (2024). Optimizing of phosphate and ammonium removal from wastewater using modified zeolite: A response surface methodology approach. Edelweiss Applied Science and Technology, 8(6), 8514-8533. https://doi.org/:10.55214/25768484.v8i6.3826

Nair, A. T., Makwana, A. R., & Ahammed, M. M. (2014). The use of response surface methodology for modelling and analysis of water and wastewater treatment processes: a review. Water science and technology, 69(3), 464-478. https://doi.org/10.2166/wst.2013.733.

Niazmand, R., Jahani, M., Sabbagh, F., & Rezania, S. (2020). Optimization of electrocoagulation conditions for the purification of table olive debittering wastewater using response surface methodology. Water, 12(6), 1687. https://doi.org/10.3390/w12061687.

Phu, T. K. C., Nguyen, P. L., & Phung, T. V. B. (2025). Recent progress in highly effective electrocoagulation-coupled systems for advanced wastewater treatment. iScience, 28(3). https://doi.org/10.1016/j.isci.2025.111965.

Salman Dawood, A., & Li, Y. (2014). Wastewater Flocculation Using a New Hybrid Copolymer: Modeling and Optimization by Response Surface Methodology. Polish Journal of Environmental Studies, 23(1).

Sarrai, A. E., Hanini, S., Merzouk, N. K., Tassalit, D., Szabó, T., Hernádi, K., & Nagy, L. (2016). Using central composite experimental design to optimize the degradation of tylosin from aqueous solution by photo-fenton reaction. Materials, 9(6), 428. https://doi.org/10.3390/ma9060428 .